

Response to the Topical Editor

Specific Comments

Question: Some of the material in the author response should be included in the paper. For example in the response to Reviewer 1: “As the national land cover data in 2000, 2005, 2010 are based on 30 m Landsat images that mainly obtained in summer season. The water surface in these datasets can be equated with annual maximum water surface results. So we compared them with our maximum ISWDC of corresponding year. The calculated R^2 is based on the area of different size of water bodies. The larger the R^2 , the better the consistency and the smaller the area error between the two datasets. Furthermore, the results of confusion matrix are equivalent to pixel scale analysis although it's not as intuitive as visual contrast.”

This makes it clearer why the maximum/summertime values are used, especially when there is a factor of 2 change in the total surface area during the course of the year (Figure 7).

Response: We added this response in Section 4.1 as a new paragraph.

Question: The comparison of the ISWDC and GSW data products has been extended to include time series of the annual size of permanent water bodies in China between 2000 and 2015 (new Figure 4 on page 12). It is not clear if water bodies below an area of 0.0625 km^2 in the GWS product have been included or not. This needs clarification.

Response: The water bodies in the GWS product with an area less than 0.0625 km^2 are not included in the comparison. We added an explanation in the first sentence in section 4.2 in order to make this question clearer.

Question: Further, as performed by Klein et al., 2017 (cited reference), an analysis could and should be made of the performance of the product for pure and mixed water pixels.

Response: In our algorithm, if the water pixel is extracted according to the principle of maximum variance between classes and minimum variance intra-class, it is recognized as pure water pixel. But in theory the most peripheral pixel of the water body must be a mixed pixel. In our product, we did not do further decomposition. In the process of accuracy evaluation, all the pixels in the center of water body and the most peripheral mixed pixels are treated as pure water. The final result of accuracy evaluation is actually the synthesis of pure water and the marginal mixed pixels. If the pure water pixels are separately evaluated, the accuracy of the results will be higher. Although the accuracy of mixed pixel regions may be reduced, but due to the proportion of mixed pixel is actually very low, we do not evaluate the precision separately.

Question: The paragraph in the final section on the overall uncertainties is simply a restatement of the results presented in Table 2.

Response: We reorganized the three paragraphs and modified some expressions on the accuracy and uncertainty analysis of the results in the final section.

Question: Finally, there would be real merit in comparing the ISWDC dataset with the Global WaterPack product of Klein et al., 2017 (cited reference) over China, especially as they are both based on MODIS imagery.

Response: Yes, indeed. Since the data produced by Igor Klein's group is not publicly shared, before we started writing this article, we had contacted the authors to obtain the data in China so we can make comparison and evaluation between the two data sets. Unfortunately, because of the post adjustment of data processing personnel, they did not provide their data eventually, so our research failed to compare with their data. If their data are publicly published in future, we will make some comparisons again.

Technical Comments

Question: Page 3: A new Table 1 has been included here in the revised manuscript.

All the following Tables (Table 1, Page 7; Table 2, Page 11 and Table 3, page 16) need to be renumbered and the references to the tables revised.

Response: We renumbered the 4 tables and revised the references of the tables in the main body of the manuscript.

Question: Page 4, line 13: “China is one of the countries that have the highest densities of rivers and lakes in the world” should be replaced by “China has one of the highest densities of rivers and lakes in the world”.

Response: We replaced the sentence of “China is one of the countries that have the highest densities of rivers and lakes in the world” by the suggested one.

Question: Page 7, Table 1: The final entry for 2015 (28) is either out of place or incorrect. Please check and amend as needed.

Response: We filled in the missing number. The correct number is 289.

Question: Page 10, lines 6-8: The 4 occurrences of “lesser than” should be the original “less than”.

Response: We corrected these misused words.

Question: Page 10, line 10: The “determinant coefficients (R^2)” should be the “coefficient of determination (R^2)”

Response: We corrected this wrong expression.

Question: Page 11: Table 2. The table second part of the caption (“the assess results”) does not make sense.

Response: We changed “the assess results” to “the accuracy evaluation results”.

Question: Page 11, line 4: Replace “whole China” with “the whole of China”. Also Page 12, caption of Figure 4.

Response: We replaced the two places with the “the whole of China”

Question: Page 15, Figure 6: It is still hard to distinguish the individual years. The use of coloured lines might provide some discrimination.

Response: We changed the lines and marks in different colors in this figure.

Question: Page 15, Figure 7: The label for the y-axis is not the “Average annual area”. It is the “area of surface water” of each region for the particular 8-day period (or similar). The precision of the numbers on the y-axis needs to be increased (0,1,1,2,2,3,3,4) -> (0,0.5,1,1.5,2,2.5,3.3,5,4).

Response: We revised the label for the y-axis as “Area of surface water” and revised the caption as “The 8-day surface water area in different regions of China”. Furthermore, the precision of numbers on the y-axis been changed as (0, 5, 10, 15, 20,).

Question: Page 19, line 18: The Gao reference is missing the journal (Remote Sensing of the Environment).

Response: We added the journal Name of “Remote Sensing of Environment”.

Question: The paper could do with a careful proof read of the English as there are other non-English constructions, e.g., neglect of the definite (the) and indefinite article (a/an).

Response: We have carefully made a proof check of the english grammer.

Time series of Inland Surface Water Dataset in China (ISWDC) for 2000-2016 derived from MODIS archives

Shanlong Lu¹, Jin Ma^{1,2}, Xiaoqi Ma^{1,3}, Hailong Tang^{1,4}, Hongli Zhao⁵, Muhammad Hasan Ali Baig⁶

¹Key Laboratory of Digital Earth Science, State Key Laboratory of Remote Sensing Science, Institute of Remote Sensing and Digital Earth, Chinese Academy of Sciences, Beijing 100094, China;

²College of Information Science and Engineering, Shandong Agricultural University, Tai'an 271018, China;

³School of Earth Sciences and Resources, China University of Geosciences, Beijing 100083, China;

⁴College of Earth Science, Chengdu University of Technology, Chengdu 610059, China;

⁵State key Laboratory of Simulation and Regulation of Water Cycle in River Basin, China Institute of Water Resources and Hydropower Research, Beijing 100038, China;

⁶Institute of Geo-Information & Earth-Observation (IGEO), PMAS Arid Agriculture University Rawalpindi, Rawalpindi 46300, Pakistan.

Correspondence to: Shanlong Lu (lusl@radi.ac.cn)

Abstract. The moderate spatial resolution and high temporal resolution of the MODIS imagery make it an ideal resource for time series surface water monitoring and mapping. We used MODIS MOD09Q1 surface reflectance archive images to create an Inland Surface Water Dataset in China (ISWDC), which maps water bodies larger than 0.0625 km² within the land mass of China for the period 2000–2016, with 8-day temporal and 250 m spatial resolution. We assessed the accuracy of the ISWDC by comparing with the national land cover derived surface water data and Global Surface Water (GSW) data. The results show that the ISWDC is closely correlated with the national reference data with ~~coefficient of determination~~**determinant coefficients** (R^2) greater than 0.99 in 2000, 2005, and 2010, while the ISWDC possess very good consistency, very similar change dynamics, and similar spatial patterns in different regions with the GSW dataset. The ISWDC dataset can be used for studies on the inter-annual and seasonal variation of the surface water systems. It can also be used as reference data for verification of the other surface water dataset and as an input parameter for regional and global hydro-climatic models. The ISWDC data are available at

1 <http://doi.org/10.5281/zenodo.2616035>.

2

3 **1 Introduction**

4 Surface water is the most important source of water from planetary water resources available for the
5 survival of both human and ecological systems (Lu and He, 2006). It is a key component of the
6 hydrological cycle and the key factor affecting the sustainable development of human society and
7 ecosystem. Both climate change and human activities have a role in affecting the surface water
8 availability at a given area and time. In order to locate the position and examine the change in dynamics
9 of the inland surface water, regional and global datasets have already been produced through remotely
10 sensed data by various researchers (Carroll et al., 2009; Verpoorter et al., 2014; Feng et al., 2015; Klein
11 et al., 2014; Tulbure et al., 2016), but these contemporary researches were limited to measuring
12 long-term changes at high spatial and temporal resolution. Pekel et al. (2016) quantified the changes in
13 global surface water (GSW) over the past 32 years (1984-2015) at 30-meters resolution by using the
14 Landsat imagery. Klein et al. (2017) generated a 250 m daily global dataset of inland water bodies based
15 on a combination of MODIS Terra and Aqua daily classifications. However, the temporal resolution of
16 the former research is near monthly, and the latter research only produced datasets from 2013-2015 ~~at~~
17 ~~the moment~~until now, while the entire MODIS archive back to July 2002 ~~–~~is still ongoing (Klein et al.,
18 2017).

19 In China numerous regional case studies have been done and produced some surface water datasets
20 but only in bits and pieces (Du et al., 2012; Lai et al., 2013; Luo et al., 2017). Their research mainly
21 focused on lakes in the Qinghai-Tibetan Plateau (Lu et al., 2017). Several research groups are focusing
22 on ~~the~~-lake water changes of this region: and have produced decadal lake surface water datasets since
23 the 1960s~~Almost every 10 year since the 1960s lake water surface area datasets have been produced~~
24 (Song et al., 2014; Zhang et al., 2014, 2017; Wan et al., 2014, 2016). At the national scale, the national

1 wetland remote sensing datasets in 1978, 1990, 2000 and 2008 (Niu et al., 2012), the national land
 2 cover datasets in 1990, 2000, 2010, and 2015 (Wu et al., 2017), and the national land use datasets in
 3 1990, 1995, 2000, 2005, 2010, 2015 (Liu et al., 2018) contain the inter-decadal or 5-year time scale
 4 water surface dataset (Table 1). However, these datasets are available with limited temporal resolution
 5 and not freely and fully shared.

6 **Table 1. National and regional surface water related datasets of China**

Dataset	Author	Time series	Resolution
Lake water surface of Tibetan Plateau	Lu et al., 2017	8-days, 2000-2012	250m
Lake surface area of Tibetan Plateau	Song et al., 2013	1970s, 1990, 2000, 2003-2009, 2011	60m, 30m
Lake area of Tibetan Plateau	Zhang et al., 2014, 2017	1970s, 1990, 2000, 2010	15m, 30m
A lake dataset for the Tibetan Plateau	Wan et al., 2014, 2016	1960s, 2005, 2014	16m, 30m
China national wetland datasets	Niu et al., 2012	1978, 1990, 2000, 2008	30 m
China national land cover datasets	Wu et al., 2017	1990, 2000, 2010, and 2015	30 m
China national land use datasets	Liu et al., 2018	1990, 1995, 2000, 2005, 2010, 2015	30m

7 The most commonly used method of water extraction is a-based on water indices ~~method~~, such as
 8 the Normalized Difference Water Index (NDWI) (Gao, 1996; McFeeters, 1996; Rogers and Kearney,
 9 2004), the Modified Normalized Difference Water Index (MNDWI) (Xu, 2006), ~~and-the~~ Automated
 10 Water Extraction Index (AWEI) (Feyisa, et al., 2014), and the Enhanced Water Index (EWI) (Wang et
 11 al., 2015). Furthermore, the single band threshold segmentation method (Li et al., 2012, Lu et al., 2017)
 12 and the multiband transformation method (Pekel et al., 2014) are also in practice. The key step for using
 13 these methods in extracting the water boundary is to determine the threshold value for segmentation.
 14 The existing threshold determination methods include human visual judgment (Huang et al., 2008; Li et
 15 al., 2012) and sample statistical analysis (Feyisa et al, 2014; Pekel etc., 2014; Pekel et al., 2016). The
 16 former relies on subjective experience, which causes the extraction results to be unstable, and thus
 17 difficult to apply on larger scales and to large volumes amounts of data. Although the latter can get more

1 accurate results through extensive sampling statistics, the use of a unified threshold for the whole image
2 or whole region may produce large errors in the local area. ~~In order to~~ overcome these problems,
3 various comprehensive classification methods are widely used. Verpoorter et al. (2014) combined the
4 Principal Component Analysis (PCA) and the Modified Brightness Index (MBI) to generate supervised
5 classes, and to divide these into water and non-water regions by using the decision tree method. Pekel et
6 al. (2016) proposed an expert system by synthetic use of a visual analytical spectral library, the NDVI
7 index, HSV transformation results, and decision tree method. Khandelwal et al. (2017) introduced a
8 global supervised classification based approach by defining initial spatial extents of each water body,
9 using the global sample datasets, and incorporating all the spectral reflectance bands of the MODIS
10 imagery. Use of supervised classification ~~and or~~ decision tree method may improve the accuracy of the
11 water surface boundary extraction, however it increases the difficulty and efficiency of the method at
12 the same time. Zhang et al. (2017) proposed an automatic threshold determination method based on the
13 LBV (L, the general radiance level; B, the visible–infrared radiation balance; V, the radiance variation
14 vector between bands) transformation of Landsat 8 OLI surface reflectance images. It was verified as an
15 accurate, simple, and robust method for surface water extraction. However, ~~the~~ cloud pixels and
16 atmospheric correction influences were not considered.

17 China has one of the highest densities of rivers and lakes in the world~~China is one of the countries~~
18 ~~that have the highest densities of rivers and lakes in the world.~~ There are more than 1500 rivers with an
19 area exceeding 1000 km², and 2928 lakes with an area larger than 1 km² ~~and giving in which form~~ a
20 total surface water area of 91,020 km² (Ma et al. 2011). However, owing to the influence of climate,
21 geography and landscape of the country, these surface water resources are unevenly distributed. They
22 are found more in the South than in the North, and more in the East than in the West. With the
23 development of the economy, the increase in the demand for industrial, agricultural and domestic water
24 has placed great pressure to these surface water systems, especially during the irrigation and drought
25 season (Gong et al., 2011; Barnett et al., 2015). Therefore, there is an urgent need for spatio-temporal

1 continuous surface water datasets to support the efficient and robust management of water resources,
2 and to investigate the relationship between the national surface water and the global climate and human
3 activities. However, until now, full public sharing data products with moderate spatial resolution and
4 near-daily temporal resolution are still lacking in China.

5 In order to address these limitations and to fulfill the need to develop a comprehensive
6 spatio-temporal dataset, this paper presents the Inland Surface Water Dataset in China (ISWDC) during
7 the period of 2000-2016 (and will be ~~continuously~~ updated continuously for the subsequent years on
8 zenodo platform), which is derived from the 8-day and 250 m spatial resolution MODIS MOD09Q1
9 product. After recalling the methodology used in surface water mapping from the MODIS MOD09Q1
10 as described by Lu et al. (2017), the precision and accuracy of the dataset are reported, including the
11 cross comparison with the existing national and global datasets.

12

13 **2 Study area and data**

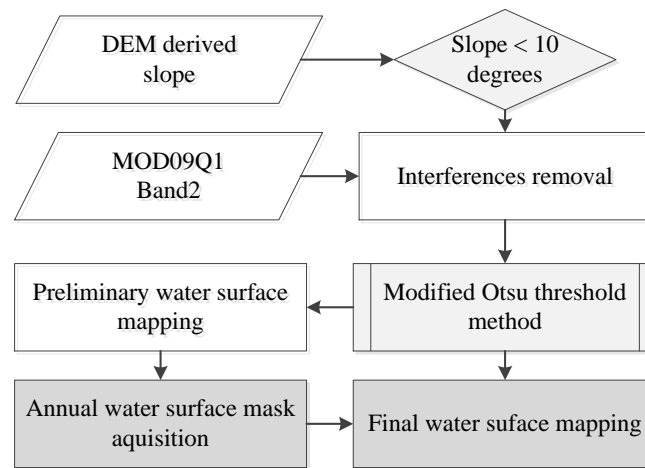
14 The inland water of this dataset refers to a water body larger than 0.0625 km² of the terrestrial land of
15 China. The MODIS MOD09Q1 imagery ~~has—been~~was used to extract surface water
16 (<https://ladsweb.modaps.eosdis.nasa.gov/search/>). MOD09Q1 is a MODIS level 3 land surface
17 reflectance product. It is an 8-day synthetic imagery of Band 1 (red band) and Band 2 (near-infrared
18 band) with the spatial resolution of 250 m. In this study the near-infrared band is directly used to extract
19 the surface water. There are 22 scenes covering the whole territory of China for every single date in a
20 form of mosaic. For the complete temporal coverage from February 24, 2000 to December 26, 2016,
21 total 16698 images were used. The SRTM (Shuttle Radar Topography Mission) DEM data with 90 m
22 spatial resolution is used as an ancillary data for surface water extraction, which is jointly ~~measured~~
23 operated by NASA-JPL (NASA Jet Propulsion Laboratory) and NIMA (National Imagery and Mapping
24 Agency (Slater et al., 2006).

1 Two types of reference dataset are used for cross comparison. The first is a derived sub-dataset of
2 surface water from China national 30 m land cover dataset of 2000, 2005 and 2010 (Liu et al., 2014;
3 Wu et al. 2017). The second is the global surface water (GSW) at ~~30-30~~-meter resolution ~~for~~ from
4 2000-2015 produced by Pekel et al. (2016).

5

6 **3 Methods**

7 The threshold segmentation method proposed by Lu et al. (2017) which employs single band with
8 one-by-one segmentation of water bodies is used to extract the surface water boundary, which includes
9 four steps: interferences removal, preliminary water surface mapping, annual water surface mask
10 acquisition, and water surface boundary extraction (Figure 1). In this study the last two steps of the
11 method are updated and improved as in following sections 3.1 and 3.2.



12

13 **Figure 1. Flowchart of the water surface extraction method reference to Lu et al. (2017)**

14 **3.1 Annual water surface mask acquisition**

15 The water surface mask is a key input data for excluding land disturbance factors that affect the
16 extraction of the water surface boundary. It is generated from the preliminary water surface mapping
17 results based on the modified Otsu threshold method applied on the selected images having less ~~er~~ cloud

1 cover and better quality in each year (Lu et al., 2017). In order to eliminate error in water area
 2 information caused by the cloud and cloud shadow in this process, the determination probability (p)
 3 parameter is used based on the fact that the cloud and its shadow will not appear in the same position
 4 for several days. The equation is as follows,

$$5 \quad \sum_{i=1}^n d_i \geq n \times p, D=1$$

6 where n is the number of the preliminary water surface mapping images, d_i is the pixel value of
 7 image i , D is the pixel value of the annual water surface mask, p is the determination probability for
 8 identifying water pixel. In this study the reference images from 2013 to 2016 were selected and the
 9 determination probability (p) was determined based on the same rule with Lu et al. (2017). Furthermore,
 10 the annual reference images and determination probability (p) of 2000-2012 are directly used here
 11 because they were originally obtained based on the whole images of China [\(Table 2\)](#).

12 **Table 12. The images used for annual water surface mask generation and the determination probability each**
 13 **year**

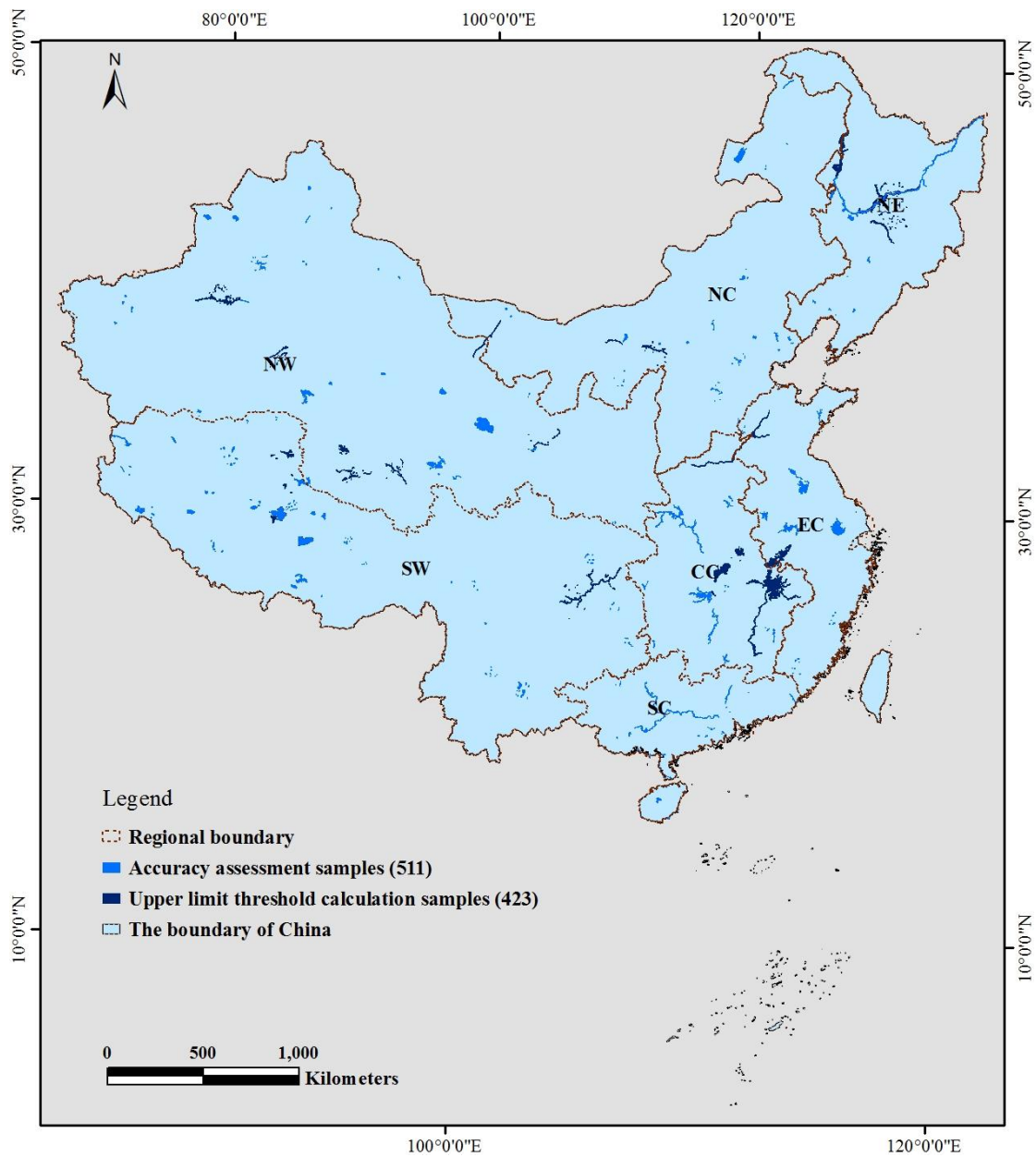
Year	Selected 8-day image dates (DOY)	Determination probability (p)
2000	185、201、209、233、241、249、257、265、281、305	0.2
2001	185、193、201、233、241、249、257、265、273、281	0.2
2002	185、193、209、217、225、233、241、249、257、265	0.2
2003	177、193、201、209、217、233、249、257、265、289	0.3
2004	185、201、217、225、233、249、257、265、273、281	0.2
2005	209、217、225、233、241、249、257、265、273、281	0.2
2006	137、145、169、177、185、193、201、209	0.2
2007	185、193、201、209、217、225、233、241、257、265	0.3
2008	193、201、209、225、233、241、249、257、265、273	0.3
2009	129、137、153、169、185、193、201、233、241、249	0.3

2010	185、209、217、225、233、241、249、257、273、281	0.2
2011	161、169、177、185、201、209、217、225、233、265	0.2
2012	185、201、209、217、225、233、241、257、265、273	0.2
2013	185、193、201、209、217、225、233、249、257、281	0.2
2014	193、201、209、225、233、241、249、265、257、273	0.3
2015	201、209、217、241、249、257、265、273、281、289	0.2
2016	193、209、225、241、257、265、273、289、305	0.2

1

2 **3.2 Final water surface mapping**

3 Before determining the threshold value for each water body in the final step of the water surface
4 extraction method (Lu et al., 2017), the average pixel value in the mask area is used to eliminate the
5 influence of the land pixels. Although this way can improve the accuracy of water surface extraction,
6 the average pixel value in different seasons will also be different. In order to optimize this process, 423
7 samples of lakes and rivers in different regions of the country are selected (Figure 2) to obtain the
8 reference average pixel value in different seasons. Two images with fewer clouds are selected for
9 each season in each year, and the average pixel values for spring, summer, and autumn are calculated
10 based on the water body samples. They were used as the upper limit threshold for determining the pixel
11 value range for the final step of water surface mapping. In the process of water turning into ice in winter,
12 the pixel value of ice is higher than that of water, and it accounts for a large proportion. The average
13 pixel value will cause the ice layer to be extracted as the water surface, the minimum pixel value of the
14 samples are used as the upper limit threshold for water surface mapping in winter. Finally, based on the
15 upper limit thresholds in different seasons each year, the final binary water surface images of different
16 time period are obtained by using the modified Otsu threshold method again (Lu et al., 2017).



1
2
3
4
5

Figure 2. The boundary of China, the accuracy assessment and the upper limit threshold calculation samples for surface water extraction. NW: Northwest China, SW: Southwest China, SC: South China, CC: Central China; NC: North China, NE: Northeast China, EC: East China.

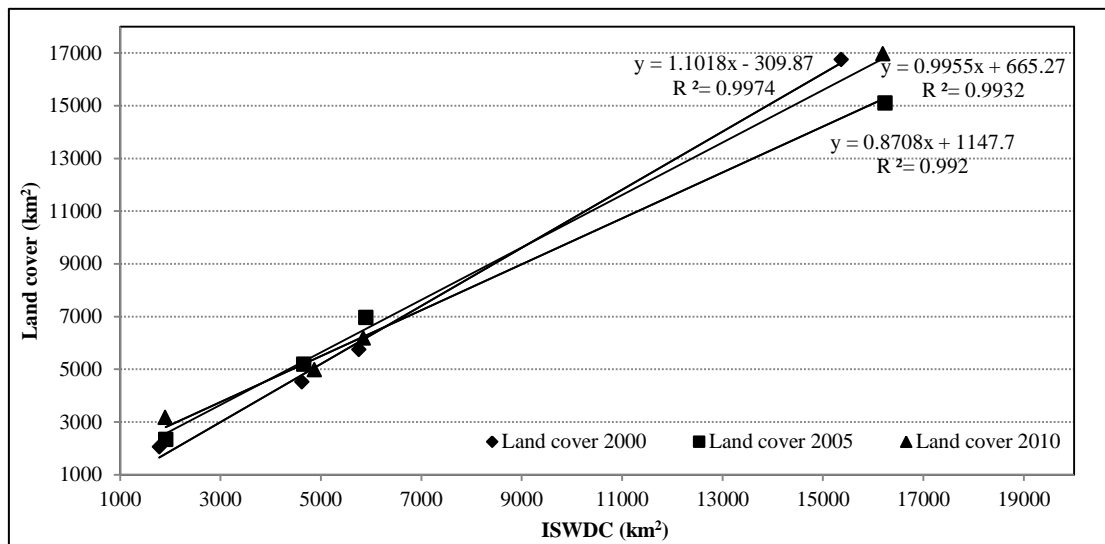
1 **4 Accuracy assessment**

2 **4.1 Comparison with the national land cover dataset**

3 Based on the 30 m resolution national land cover dataset of 2000, 2005, and 2010, 511 samples from
4 lakes and rivers spreading out across the country are selected as ground truth data (Figure 2), including
5 11 very large water bodies with areas larger than 1000 km², 12 large water bodies with areas larger than
6 500 km² and less~~er~~ than 1000 km², 29 medium sized water bodies with area larger than 100 km² and
7 less~~er~~ than 500 km², and 459 smaller water bodies with areas less~~er~~ than 100 km². They were compared
8 with the maximum ISWDC in the corresponding years.

9 The results show that the ISWDC are highly consistent with the reference land cover derived surface
10 water data. The ~~coefficient of determination~~~~determinant coefficients~~ (R^2) in 2000, 2005 and 2010 are
11 found to be 0.9974, 0.992, and 0.9932, respectively as shown in Figure 3. The confusion matrix analysis
12 results show that the average user accuracy is 91.13%, the average producer accuracy is 88.95%, and
13 the average Kappa coefficient is 0.88 in three years (Table ~~23~~).

14 As the national land cover data in 2000, 2005, 2010 are based on 30 m Landsat images that mainly
15 obtained in summer season. The water surface in these datasets can be equated with annual maximum
16 water surface results. So we compared them with our maximum ISWDC of corresponding year. The
17 calculated R^2 is based on the area of different size of water bodies. The larger the R^2 , the better the
18 consistency and the smaller the area error between the two datasets. Furthermore, the results of
19 confusion matrix are equivalent to pixel scale analysis although it is not as intuitive as visual contrast.



1

2 **Figure 3.** Comparison of the total area of surface water body samples with different size (< 100 km², 100-500 km², 500-1000
3 km², >1000 km²) between ISWDC and the National land cover derived surface water data.

4

Table 23. Accuracy analysis samples in different region and the assess-accuracy evaluation results

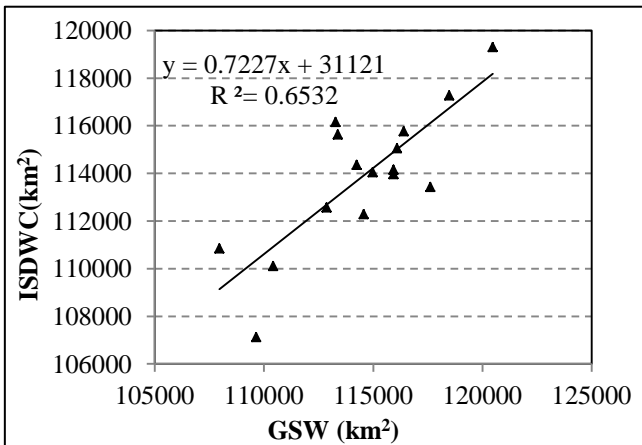
Sample regions	Sample water bodies				
	Very large	Large	Medium	Small	Total
North China (NC)	1	1	1	73	76
Northeast China (NE)	1	2	2	21	26
East China (EC)	2	1	3	34	40
Southwest China (SW)	2	3	5	75	85
Northwest China (NW)	2	2	13	166	183
Central China (CC)	2	1	2	46	51
South China (SC)	1	2	3	44	50
Average user accuracy	96.14	94.75	93.69	79.96	91.13
Average producer accuracy	92.64	88.87	92.69	81.60	88.95
Average Kappa coefficient	0.94	0.93	0.93	0.72	0.88

1

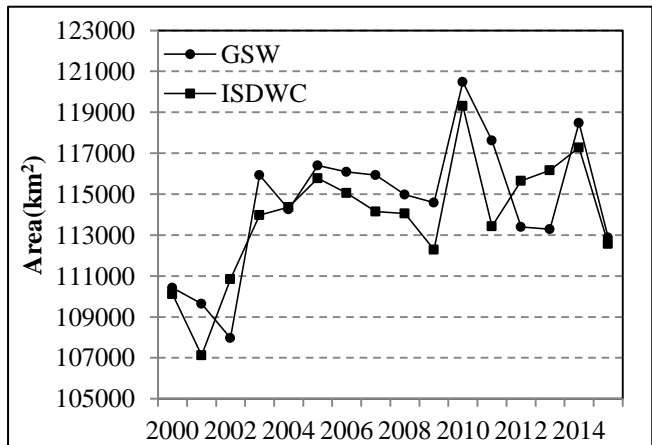
2 4.2 Assessment against the global surface water dataset

3 The time series of annual ISWDC and GSW permanent water bodies with an area larger than 0.0625
4 km² of the whole of China from 2000-2015 were also compared. The results show that the two datasets
5 possess very good consistency (R²=0.6532) (Figure 4a) and very similar change dynamics (Figure 4b).

6 The annual ISWDC and GSW permanent water bodies ~~with area larger than 0.0625 km²~~-in 2015 also
7 indicate similar spatial patterns in different regions (Figure 5). For the lake groups in central
8 Qinghai-Tibetan Plateau, the comparison between ISWDC obtained from MODIS and Landsat derived
9 GSW indicated a closer pattern between the two results (Figure 5a). For the rivers and lakes interlaced
10 with Poyang Lake region, in addition to the narrow width of the river and some small water bodies, the
11 coincidence between the two datasets is also very high (Figure 5b). The over-extracted water (red
12 regions in Figure 5) on the margins for large water bodies like Siling Co, Namco, Poyang Lake, and
13 some of the wide rivers, and the under-extracted slender rivers and small water bodies (green regions in
14 Figure 5), for the ISWDC dataset, are mainly caused by the mixed pixel effects due to relatively coarse
15 spatial resolution of the MODIS images.



16 (a)



17 (b)

18

18 Figure 4. Comparison of the time series annual ISWDC and GSW permanent water bodies of the whole of China from 2000-2015.

1 (a) is the correlation analysis result, (b) is the change trend comparison result.

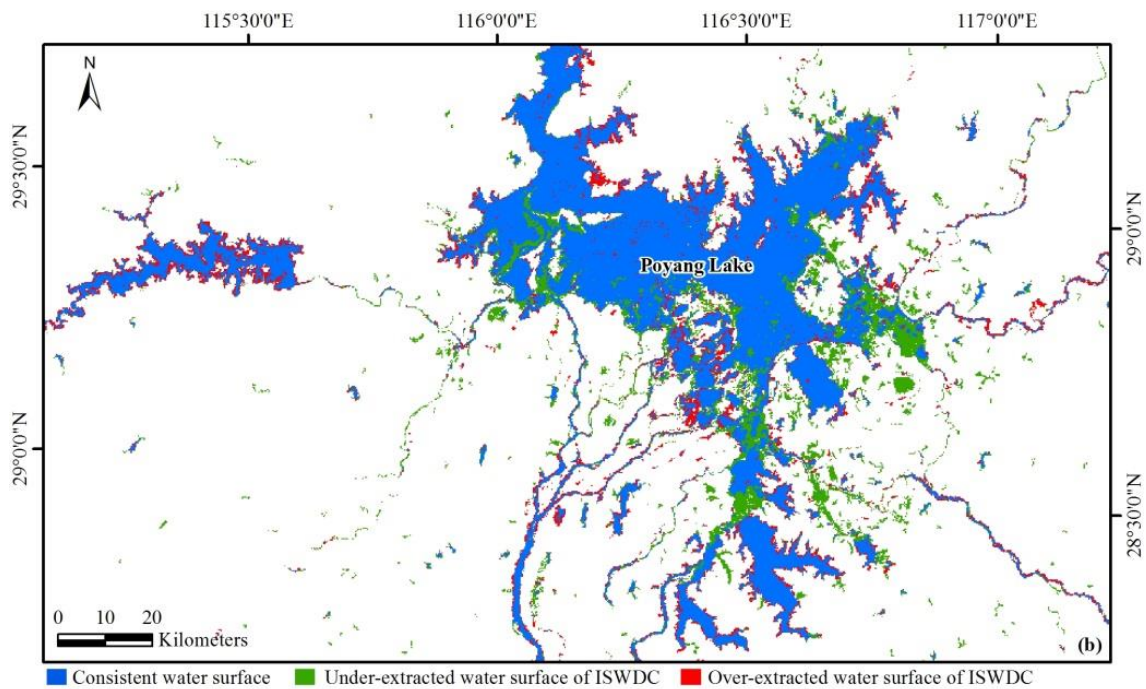
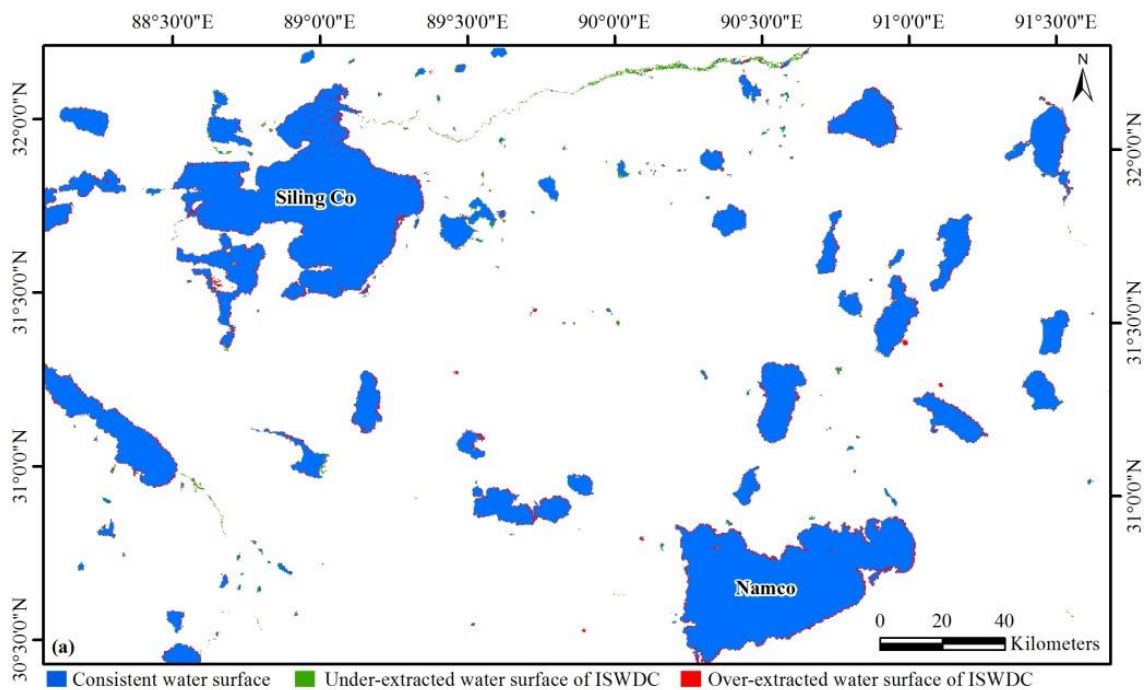


Figure 5. Comparison of permanent water bodies derived from ISWDC and GSW over the sites of the central Qinghai-Tibetan

1 Plateau (a) and Poyang Lake region (b).

2

3 **5 Applications and data availability**

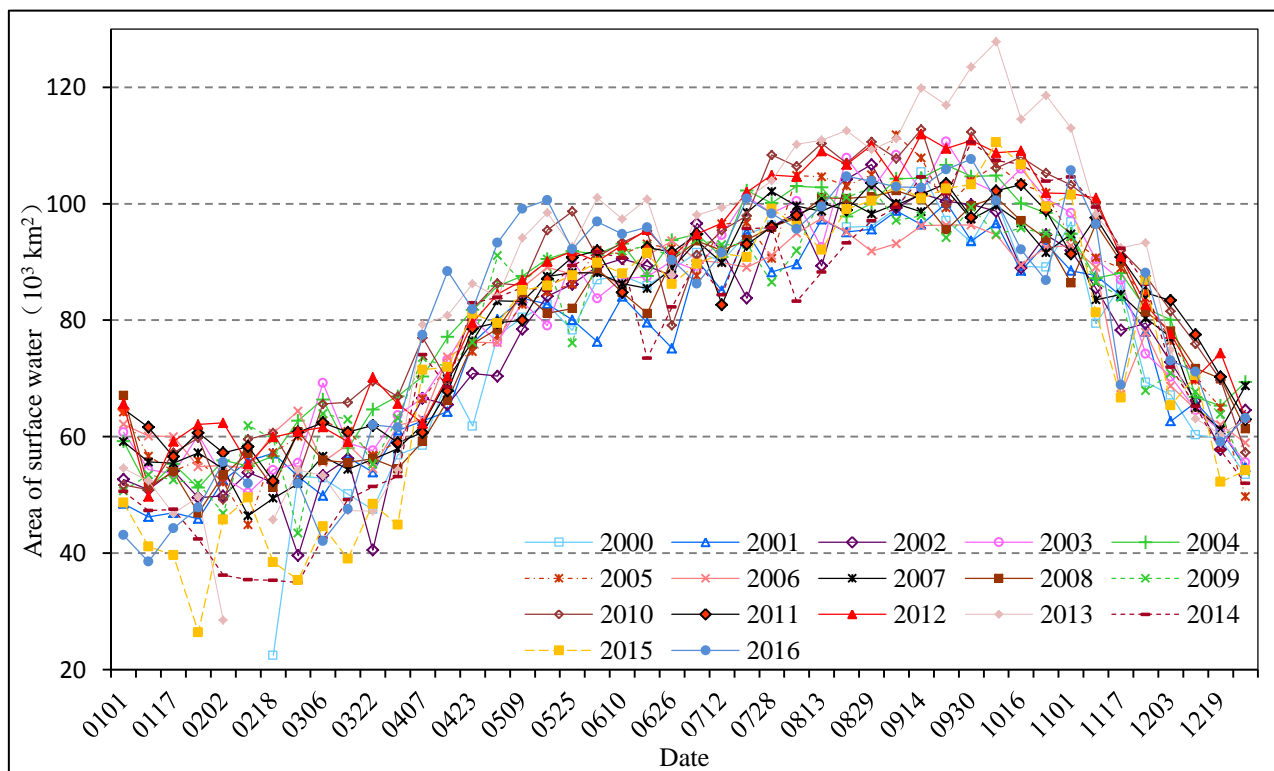
4 **5.1 Time series of surface water dataset applications**

5 Time series of surface water dataset can be used to analyze the inter-annual and seasonal variation
6 characteristics of surface water area, including inter-annual variation trend, abrupt change time,
7 intra-annual hydrological process monitoring etc. (Huang et al., 2018; Xing et al., 2018). Similarly, it
8 can also be used as cross-validation reference data for global surface water datasets with a similar
9 spatial resolution (Klein et al., 2017), and as a key input parameter for regional and global
10 hydro-climatic model calibration and evaluation (Khan et al., 2011; Stacke and Hagemann, 2012).

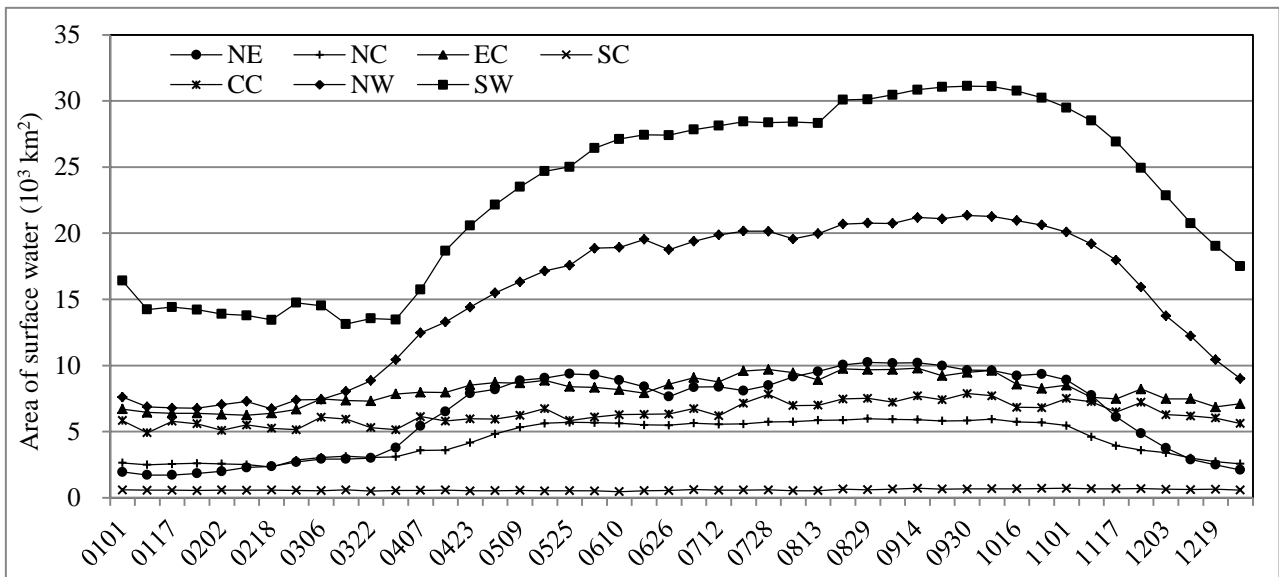
11 For example, based on the ISWDC from 2000-2016, the annual variation of surface water in China
12 can be obtained by superimposing all the 8-day time series water surface area data of each year. Figure
13 6 shows that the surface water area began to increase in early March and increased gradually in spring
14 and summer. After ~~reached~~reaching its peak in autumn, it then began to decrease gradually. The annual
15 variation of surface water area in different regions can also be portrayed by calculating the multi-year
16 average of every 8-day data. Figure 7 shows that the surface water area of Southwest China (SW) and
17 Northwest China (NW) is very large and inter-seasonally it varies greatly than the surface water area of
18 other regions. Surface water area in Northeast China (NE) began to increase rapidly in spring. It reached
19 a peak in May and decreased slightly in June-July. After reaching its maximum in August-September, it
20 began to decline again in October. In North China (NC), surface water area is relatively small, but the
21 change still shows some seasonality. There is a significant increase in summer and autumn, but the
22 range of increase and decrease is relatively small. Surface water area in Central China (CC) and Eastern
23 China (EC) varies steadily during the year. It reaches its maximum in summer and begins to decrease
24 gradually in late summer and early autumn. Surface water area in South China (SC) was relatively

1 stable throughout the year.

2 Furthermore, the spatial distributions of surface water can clearly be depicted by means of multi-year
3 average analysis. The results in Table 34 show that surface water of inland China is mainly distributed
4 in western China, accounting for 49.13% of the total surface water area, with 29.88% in the Southwest
5 China (SW) and 19.25% in the Northwest China (NW), followed by the Central China (CC) and East
6 China (EC), which accounted for 8.13% and 24.78% of the total surface water area, respectively. The
7 North China (NC), Northeast China (NE) and South China (SC) account for the other 17.96% of the
8 national surface water area.



10
11
Figure 6. Annual change of total water area during the period of 2000-2016.



1
2
3
4
5

Figure 7. The 8-day surface water area in different regions of China Average annual 8-day surface water area of different regions of China from 2000 to 2016. NE: Northeast China, NC: North China, EC: East China, SC: South China, CC: Central China, NW: Northwest China, SW: Southwest China.

Table 34. The average distribution of surface water area in inland China from 2000-2016

Regions	Area(km ²)	Area percentage (%)
North China (NC)	6250.6	6.11
Northeast China (NE)	8991.3	8.79
East China (EC)	25342.3	24.78
Central China (CC)	9313.4	8.13
South China (SC)	3126.0	3.06
Southwest China (SW)	30548.6	29.88
Northwest China (NW)	19680.2	19.25
Total	103252.3	100.00

6
7

5.2 Data availability

1 The ISWDC dataset is distributed under a Creative Commons Attribution 4.0 License. The data may be
2 downloaded from the data repository Zenodo at <http://doi.org/10.5281/zenodo.2616035> (Lu et al., 2019).
3 In each 8-day surface water image, the pixel values of 1 and 0 represent the water and the background
4 respectively. The 8-day data in each month can be used to calculate the monthly water occurrence and
5 all the 8-day data in each year can be used to calculate the yearly water occurrence, by summing up all
6 the surface water images together in corresponding time periods. The vector datasets of the 8-day
7 surface water boundaries extracted from the raster data products can also be obtained through the same
8 link.

9

10 **6. Discussion and conclusions**

11 In this study, the 8-day 250-meter resolution surface water dataset of inland China (ISWDC) from 2000
12 to 2016 has been introduced. It is a fully public sharing data product with prominent features of long
13 time series, moderate spatial resolution and high temporal resolution. The ISWDC is a valuable basic
14 data source for the analysis of ~~the~~ dynamic changes of surface water in China in the past 20 years. ~~---~~

15 The results have been validated based on the 2000, 2005 and 2010 national land cover derived
16 surface water data and show high accuracy~~The accuracy analysis results show that the ISWDC is highly~~
17 ~~consistent with the national land cover derived surface water data from 2000, 2005 and 2010, with the~~
18 ~~determinant coefficients (R^2) of 0.9974, 0.992, and 0.9932 respectively. The average user accuracy is~~
19 ~~91.13%, the average producer accuracy is 88.95%, and the average Kappa coefficient is 0.88 for these~~
20 ~~three years. Furthermore, a comparison with the GWS service underlines the reliability of temporal~~
21 ~~processes and spatial distribution. ~~in~~In terms of temporal variation, the ISWDC and the GWS possess~~
22 ~~excellent consistency and very similar change dynamics during the whole time period, which simply~~
23 ~~shows that both datasets are highly correlated. For the spatial distribution characteristics, the ISWDC in~~
24 ~~2015 has similar spatial patterns in different regions (including the central Qinghai-Tibetan Plateau and~~

1 ~~Poyang Lake region~~) to that of the GSW dataset, especially for larger water bodies, ~~(such as lakes,~~
2 ~~water reservoirs and wide rivers).~~

3 The advantage of the ISWDC dataset is its high level of revealing the spatio-temporal variability of
4 inland surface water. ~~Based on the ISWDC for 2000-2016,~~ ~~Based on this dataset,~~ the spatial
5 distribution characteristics and temporal variation processes of surface water can be described through
6 the multi-year average spatial statistics and annual data overlapping analysis. In addition, the dataset
7 can also be used as a cross-validation reference data for other global surface water datasets, and a key
8 input parameter for regional and global hydro-climatic models.

9 However influenced by the algorithm design and the used data sources the results have certain
10 limitations. First of all, as for other surface water datasets derived from multi-spectral sensors, it only
11 includes open water surfaces, while water bodies which are covered by vegetation are not captured.

12 Secondly, ~~A~~ as ISWDC only uses MODIS MOD09Q1 near-infrared band for water surface extraction,
13 thus the accuracy of datasets depends mainly on the quality of the original 8-day synthetic images.
14 When there ~~are exist~~ clouds exist in the water distribution region ~~in of~~ the synthetic image at a certain
15 time, the cloud covered water surface will not be extracted which causes underestimation for extracting
16 water bodies. In addition, the reference images used to produce the annual water surface mask will also
17 affect the accuracy of the final results. For example, if the selected image does not contain the
18 information of the actual maximum water surface occurrence in that year, it may lead to the exclusion of
19 that part of the water pixels which lies outside the mask. ~~Finally~~ ~~Furthermore~~, because of the small
20 difference of reflectance between the ice-water mixing boundary in autumn and spring, the accuracy of
21 water surface area extraction will be limited in these two seasons.

22 Although the water surface extraction method designed in this study is aimed at extracting water
23 surface information from the MODIS MOD09Q1 images, its core process is automatic thresholding for
24 estimation of water bodies one by one. Therefore, this method is also applicable to traditional water
25 body indices, such as NDWI, MNDWI and AWEL, or to other water surface information based on

1 enhanced thematic data. In the future, while continuing to extend the existing datasets from 2017 to now
2 by using this method, the 30-meter GWS dataset in China will be extended. At the same time, the
3 national 10-meter spatial resolution water surface dataset based on Sentinel-2 imagery will be produced.
4 After the national scale datasets are completed, the corresponding global scale datasets are also
5 expected.

6
7 **Author contributions.** SL supervised the downloading and processing of satellite images and designed the
8 methodology. JM contributed to downloading, processing satellite images, and extracting the surface water data
9 (ISWDC). XM extracted the reference surface water data from the national land cover datasets and analyzed the
10 accuracy of the ISWDC. HT extracted the Global Surface Water (GSW) from the Google Earth Engine platform. HL
11 made contribution for manuscript structure design and revision. MHAB optimized article structure, figures and English
12 grammar. All authors have read and approved the final paper.

13
14 **Acknowledgements.** We thank the National Key Research and Development Program of China (2017YFC0405802,
15 2016YFC0503507-03), the Key Program of the National Natural Science Foundation of China (91637209), the project
16 of China geological survey (DD20160106), and the Strategic Priority Research Program of the Chinese Academy of
17 Sciences (XDA19070201) for financial support. We thank NASA EOSDIS LAADS DAAC platform
18 (<https://ladsweb.modaps.eosdis.nasa.gov/>) and NASA-JPL and NIMA for providing the MODIS and SRTM datasets.
19 We also thank JRC and Google Earth Engine (<https://earthengine.google.com>) for providing the Global Surface Water
20 (GSW) dataset.

21 22 **References**

23 Barnett, J., Rogers, S., Webber, M., Finlayson, B., and Wang, M.: Transfer project cannot meet China's water needs,
24 *Nature*, 527, 295–297, <https://doi.org/10.1038/527295a>, 2015.
25 Carroll, M.L., Townshend, J.R., DiMiceli, C.M., Noojipady, P., and Sohlberg, R.A.: A new global raster water mask at

1 250 m resolution, International Journal of Digital Earth, 2, 291–308, <http://dx.doi.org/10.1080/17538940902951401>,
2 2009.

3 Du, Z., Bin, L., Ling, F., Li, W., Tian, W., Wang, H., Gui, Y., Sun, B., and Zhang, X.: Estimating surface water area
4 changes using time-series Landsat data in the Qingjiang River Basin, China, Journal of Applied Remote Sensing, 6,
5 3609, <https://doi.org/10.1117/1.JRS.6.063609>, 2012.

6 Feng, M., Sexton, J.O., Channan, S., and Townshend, J.R.: A global, high-resolution (30-m) inland water body dataset
7 for 2000: first results of a topographic–spectral classification algorithm, International Journal of Digital Earth, 1–21,
8 <http://dx.doi.org/10.1080/17538947.2015.1026420>, 2015.

9 Feyisa, G.L., Meilby, H., Fensholt, R. and Proud, S. R.: Automated Water Extraction Index: A new technique for
10 surface water mapping using Landsat imagery, Remote Sensing of Environment, 140, 23–35,
11 <http://dx.doi.org/10.1016/j.rse.2013.08.029>, 2014.

12 Gao, B.: NDWI A Normalized Difference Water Index for Remote Sensing of Vegetation Liquid Water From Space,
13 [Remote Sensing of Environment](https://doi.org/10.1016/S0034-4257(96)00067-3), 266, 257–266, [https://doi.org/10.1016/S0034-4257\(96\)00067-3](https://doi.org/10.1016/S0034-4257(96)00067-3), 1996.

14 Gong, P., Yin, Y., and Yu, C.: China: Invest Wisely in Sustainable Water Use, Science, 331, 1264–1265,
15 <https://doi.org/10.1126/science.331.6022.1264-b>, 2011.

16 Huang, C., Chen, Y., Zhang, S., and Wu, J.: Detecting, extracting, and monitoring surface water from space using
17 optical sensors: A review, Reviews of Geophysics, 56, <https://doi.org/10.1029/2018RG000598>, 2018.

18 Huang, H., Zhao, P., Chen, Z., and Guo, W.: Research on the method of extracting water body information from
19 ASTER remote sensing image, Remote Sensing Technology and Application, 23, 525–528,
20 <https://doi.org/10.11873/j.issn.1004-0323.2008.5.525>, 2008.

21 Khan, S.I., Hong, Y., Wang, J., Yilmaz, K.K., Gourley, J.J., Adler, R.F., Brakenridge, G.R. Habib, S., and Irwin, D.:
22 Satellite Remote Sensing and Hydrologic Modeling for Flood Inundation Mapping in Lake Victoria Basin:
23 Implications for Hydrologic Prediction in Ungauged Basins, IEEE TRANSACTIONS ON GEOSCIENCE AND
24 REMOTE SENSING, 49, 85–95, <https://doi.org/10.1109/TGRS.2010.2057513>, 2011.

25 Khandelwal, A., Karpatne, A., Marlier, M.E., Kim, J., Lettenmaier, D.P., and Kumar, V.: An approach for global
26 monitoring of surface water extent variations in reservoirs using MODIS data, Remote Sensing of Environment, 202,
27 113–128, <http://dx.doi.org/10.1016/j.rse.2017.05.039>, 2017.

- 1 Klein, I., Dietz, A.J., Gessner, U., Galayeva, A., Myrzakhmetov, A., and Kuenzer, C.: Evaluation of seasonal water
2 body extents in Central Asia over the past 27 years derived from medium-resolution remote sensing data,
3 International Journal of Applied Earth Observation and Geoinformation, 26, 335–349,
4 <http://dx.doi.org/10.1016/j.jag.2013.08.004>, 2014.
- 5 Klein, I., Gessner, U., Dietz, A.J., and Kuenzer, C.: Global WaterPack – A 250 m resolution dataset revealing the daily
6 dynamics of global inland water bodies, Remote Sensing of Environment, 198, 345–362,
7 <http://dx.doi.org/10.1016/j.rse.2017.06.045>, 2017.
- 8 Lai, Y., Qiu, Y., Fu, W., and Shi, L.: Monitoring and analysis of surface water in Kashgar region based on TM imagery
9 in last 10 years, Remote Sensing Information, 28, 50–57, <https://doi.org/10.3969/j.issn.1000-3177.2013.03.009>,
10 2013.
- 11 Li, X., Xiao, J., Li, F., Xiao, R., Xu, W., and Wang, L.: Remote Sensing monitoring of the Qinghai Lake based on EOS
12 /MODIS data in recent 10 years, Journal of Natural Resources, 22, 1962–1970,
13 <http://www.jnr.ac.cn/CN/10.11849/zrzyxb.2012.11.015>, 2012.
- 14 Liu, J., Kuang, W., Zhang, Z., Xu, X., Qin, Y., Ning, J., Zhou, W., Zhang, S., Li, R., Yan, C., Wu, S., Shi, X., Jiang, N.,
15 Yu, D., Pan, X., and Chi, W.: Spatiotemporal characteristics, patterns and causes of land use changes in China since
16 the late 1980s, ACTA GEOGRAPHICA SINICA, 69, 3–14, <https://doi.org/10.1007/s11442-014-1082-6>, 2014.
- 17 Liu, J., Jia, N., Kuang, W., Xu, X., Zhang, S., Yan, C., Li, R., Wu, S., Hu, Y., Du, G., Chi, W., Pan, T., and Ning, J.:
18 Spatio-temporal patterns and characteristics of land-use change in China during 2010–2015, ACTA
19 GEOGRAPHICA SINICA, 73, 789–802, <https://doi.org/10.11821/dlxb201805001>, 2018.
- 20 Lu, G., and He, H. ~~2006~~: View of global hydrological cycle ~~-,~~ Advances in water science, 17 ~~(3)~~ ~~-,~~ 419–424 ~~-,~~ 2006.
- 21 Lu, S., Ma, J., Ma, X., Tang, H., Zhao, H., and Ali Bai Hasan, M.: Time series of Inland Surface Water Dataset in
22 China (ISWDC) [Dataset], Zenodo, <http://doi.org/10.5281/zenodo.2616035>, 2019.
- 23 Lu, S., Jia, L., Zhang, L., Wei, Y., Baig, M., Zhai, Z., Ment, J., Li, X., and Zhang, G.: Lake water surface mapping in
24 the Tibetan Plateau using the MODIS MOD09Q1 product, Remote Sensing Letters, 8, 224–233,
25 <http://dx.doi.org/10.1080/2150704X.2016.1260178>, 2017.
- 26 Luo, C., Xu, C., Cao, Y., and Tong, L.: Monitoring of water surface area in Lake Qinghai from 1974 to 2016, Journal
27 of Lake Sciences, 29, 1245–1253, <https://doi.org/10.18307/2017.0523>, 2017.

- 1 Ma, R., Yang, G., Duan, H., Jiang, J., Wang, S., Feng, X., Li, A., Kong, F., Xue, B., Wu, J., and Li, S.: China's lakes at
2 present: Number, area and spatial distribution, *Science China Earth Sciences*, 394–401,
3 <https://doi.org/10.1007/s11430-010-4052-6>, 2011.
- 4 McFeeters, S.K.: The use of the Normalized Difference Water Index (NDWI) in the delineation of open water features,
5 *International Journal of Remote Sensing*, 17, 1425–1432, <http://dx.doi.org/10.1080/01431169608948714>, 1996.
- 6 Niu, Z., Zhang, H., Wang, X., Yao, W., Zhou, D., Zhao, K., Zhao, H., Li, N., Huang, H., Li, C., Yang, J., Liu, C., Liu,
7 S., Wang, L., Li, Z., Yang, Z., Qiao, F., Zheng, Y., Chen, Y., Sheng, Y., Gao, X., Zhu, W., Wang, W., Wang, H., Weng,
8 Y., Zhuang, D., Liu, J., Luo, Z., Cheng, X., Guo, Z., and Gong, P.: Mapping Wetland Changes in China between
9 1978 and 2008, *Chinese Science Bulletin*, 57, 1400–1411, <https://doi.org/10.1007/s11434-012-5093-3>, 2012.
- 10 Pekel, J., Vancutsem, C., Bastin, L., Clerici, M., Vanbogaert, E., Bartholome, E., and Defourny, P.: A near real-time
11 water surface detection method based on HSV transformation of MODIS multi-spectral time series data, *Remote
12 Sensing of Environment*, 140, 704–716, <https://doi.org/10.1016/j.rse.2013.10.008>, 2014.
- 13 Pekel, J.F., Cottam, A., Gorelick, N., and Belward, A.S.: High-resolution mapping of global surface water and its
14 long-term changes, *Nature*, 540, 418–422, <https://doi.org/10.1038/nature20584>, 2016.
- 15 Rogers, A.S., and Kearney, M.S.: Reducing signature variability in unmixing coastal marsh Thematic Mapper scenes
16 using spectral indices, *International Journal of Remote Sensing*, 20, 2317–2335,
17 <https://doi.org/10.1080/01431160310001618103>, 2004.
- 18 Song, C., Huang, B., Ke, L., and Richards, K.S.: Remote sensing of alpine lake water environment changes on the
19 Tibetan Plateau and surroundings: A review, *ISPRS Journal of Photogrammetry and Remote Sensing*, 92, 26–37,
20 <http://dx.doi.org/10.1016/j.isprsjprs.2014.03.001>, 2014.
- 21 Stacke, T., and Hagemann, S.: Development and evaluation of a global dynamical wetlands extent scheme, *Hydrology
22 and Earth System Sciences*, 16, 2915–2933, <https://doi.org/10.5194/hess-16-2915-2012>, 2012.
- 23 Tulbure, M.G., Broich, M., Stehman, S.V., and Kommareddy, A.: Surface water extent dynamics from three decades of
24 seasonally continuous Landsat time series at subcontinental scale in a semi-arid region, *Remote Sensing
25 Environment*, 178, 142–157, <https://doi.org/10.1016/j.rse.2016.02.034>, 2016.
- 26 Verpoorter, C., Kutser, T., and Tranvik, L.: Automated mapping of water bodies using Landsat multispectral data,
27 *Limnology and Oceanography: Methods*, 10, 1037–1050, <https://doi.org/10.4319/lom.2012.10.1037>, 2012.

- 1 Verpoorter, C., Kutser, T., Seekell, D.A., and Tranvik, L.J.: A global inventory of lakes based on high-resolution
2 satellite imagery, *Geophysical Research Letters*, 41, 6396–6402, <https://doi.org/10.1002/2014GL060641>, 2014.
- 3 Wan, W., Xiao, P., Feng, X., Li, H., Ma, R., Duan, H., and Zhao, L.: Monitoring lake changes of Qinghai-Tibetan
4 Plateau over the past 30 years using satellite remote sensing data, *Chinese Science Bulletin*, 59, 1021–1035,
5 <https://doi.org/10.1007/s11434-014-0128-6>, 2014.
- 6 Wan, W., Long, D., Hong, Y., Ma, Y., Yuan, Y., Xiao, P., Duan, H., Han, Z., and Gu, X.: A lake dataset for the Tibetan
7 Plateau from the 1960s, 2005, and 2014, *Scientific data*, 3, 160039, <https://doi.org/10.1038/sdata.2016.39>, 2016.
- 8 Wang, J., Sheng, Y. and Tong, T.S.D.: Monitoring decadal lake dynamics across the Yangtze Basin downstream of
9 Three Gorges Dam, *Remote Sensing of Environment*, 152, 251–269, <https://doi.org/10.1016/j.rse.2014.06.004>,
10 2014.
- 11 [Wang, S., Baig, M. H. A., Zhang, L., Jiang, H., Ji, Y., Zhao, H., and Tian, J.: A Simple Enhanced Water Index \(EWI\)](#)
12 [for Percent Surface Water Estimation Using Landsat Data, Selected Topics in Applied Earth Observations and](#)
13 [Remote Sensing, IEEE Journal of, 8, 90–97, https://doi.org/10.1109/JSTARS.2014.2387196, 2015.](#)
- 14 Wang, X., Xie, S., Zhang, X., Chen, C., Guo, H., Du, J., and Duan, Z.: A robust Multi-Band Water Index (MBWI) for
15 automated extraction of surface water from Landsat 8 OLI imagery, *International Journal of Applied Earth*
16 *Observation and Geoinformation*, 68, 73–91, <https://doi.org/10.1016/j.jag.2018.01.018>, 2018.
- 17 Wu, B., Bao, A., Chen, J., Huang, J., Li, A., Liu, C., Ma, R., Wang, Z., Yan, C., Yu, X., Zeng, Y., and Zhang L.: Land
18 cover in China, Beijing: Science Press, in Chinese, 2017.
- 19 Xing, L., Tang, X., Wang, H., Fan, W., and Wang, G.: Monitoring monthly surface water dynamics of Dongting Lake
20 using Sentinel-1 data at 10 m, *PeerJ*, 6, e4992, <https://doi.org/10.7717/peerj.4992>, 2018.
- 21 Xu, H.Q.: Modification of normalized difference water index (NDWI) to enhance open water features in remotely
22 sensed imagery, *International Journal of Remote Sensing*, 27, 3025–3033,
23 <https://doi.org/10.1080/01431160600589179>, 2006.
- 24 Zhang, G., ~~F.~~ Yao T., ~~H.~~ Xie, H., ~~K.~~ Zhang, K., and Zhu, F.: ~~Zhu~~. Lakes' State and Abundance across the Tibetan
25 Plateau, *Chinese Science Bulletin*, 59, 3010–3021, <https://doi.org/10.1007/s11434-014-0258-x>, 2014.
- 26 Zhang, G., Li, J., and Zheng, G.: Lake-area mapping in the Tibetan Plateau: an evaluation of data and methods,
27 *International Journal of Remote Sensing*, 38, 742–772, <https://doi.org/10.1080/01431161.2016.1271478>, 2017.

1 Zhang, T., Ren, H., Qin, Q., Zhang, C., and Sun, Y.: Surface Water Extraction From Landsat 8 OLI Imagery Using the
2 LBV Transformation, IEEE JOURNAL OF SELECTED TOPICS IN APPLIED EARTH OBSERVATIONS AND
3 REMOTE SENSING, 10, 4417–4429, <https://doi.org/10.1109/JSTARS.2017.2719029>, 2017.